All-optical performing of logic-based operations due to a two-phonon light scattering

A.S. Shcherbakov, E. Tepichin Rodríguez, A. Aguirre López.
National Institute for Astrophysics, Optics and Electronics,
Apartado postal 51 y 216, Puebla, Pue., 72000 Mexico,
Tel. +52 (222) 2472940
e-mail: alex@inaoep.mx,
e-mail: tepichin@inaoep.mx,
e-mail: aaguirre@inaoep.mx.

Recibido el 10 de enero de 2003; aceptado el 1 de septiembre de 2003

We describe physical principles of a two-phonon light scattering in crystals and present the feasibility of exploiting such a phenomenon for the creation of an all-optical logic. Both performing the functionally complete set of logic operations and fulfilling one bit memory have been algorithmically analyzed and estimated.

Keywords: Two-phonon light scattering; all-optical logic.

En el presente artículo se discuten los principios físicos de la difracción de la luz por dos fotones en cristales y se presenta la posibilidad de explotar tal fenómeno para la creación de lógica todo-óptica. Se presenta tanto un conjunto completo de operaciones lógicas como la realización de una memoria de un solo bit, que han sido estimadas y analizadas algorítmicamente.

Descriptores: Esparcimiento de la luz por dos fonones; lógica todo-óptica

PACS: 42.25.Fx; 42.79.Ta

1. Introduction

One of the avenues in modern optical computing is connected with performing digital computations, in particular, logic operations using opto-electronic components [1]. As a rule, up-to-date digital data processing systems exploit the components whose individual speed of operation is about of 10^{-9}s. In the context of increasing the bit-rate essentially the components, eliminating any photon-electron conversions and operating in fact all-optically, have to be developed and potentially exploited in digital data processing. At present, a few types of all-optical devices, performing the logic operations, are well known. For instance, the logic gates based on dispersive or absorptive nonlinearity in Fabry-Perot cavities [2] as well as fiber logic gates, using the effect of stimulated Raman scattering [3] or Kerr nonlinearity in Sagnac and Mach-Zender interferometers [4]. A scheme of all-optical time division demultiplexing module, combining the technology of all-optical saturable absorbers and the diffractive optics [5], as well as the effects of spatial chirp of the built-in low-power switching in grating on the spectral range and switching power of all-optical switching in active semiconductors periodic structures [6] should be pointed out. To realize binary logic operations in optics a lot of various physical mechanisms can be used, but they all lead to input-output functions, which are identical by a large margin. Evidently, performing binary logic operations can be provided by the logic gates, whose input-output functions manifest local nonlinearity. A generalized schematic arrangement and the principle of operation for binary logic gates are illustrated in Fig. 1. At first, two input optical intermediate binary (that is to say two-level) signals, representing 0 or 1, add together to give a next three-level signal, whose value is equal to the number of inputs with logic unities. Then, this signal converts by nonlinear function into output binary (or two-level) signal.

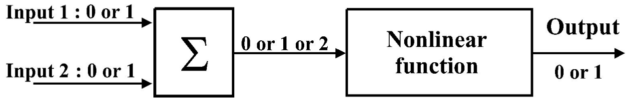

FIGURE 1. Generalized functional scheme of binary logic gate with two inputs.

In optics, the zero-level signal is usually represented by low intensity light beam, while the unity-level signal is represented by high intensity one. Addition proceeds by the superposition of optical signals. There are 16 feasible binary logic operations with two input signals and one output signal, but only 8 of them are commutative in reference to the input signals, *i.e.*, they have functionally indistinguishable inputs. Some of nonlinear input-output functions, conforming to commutative binary logic operations, are presented in Fig. 2. A set of simple logic operations is complete, when this set gives us a possibility to create an arbitrary logic circuit. For binary systems, two pairs of logic operations: (NOT, AND) and (NOT, OR) presents examples of such complete sets. These pairs of operations can be united into one gate, performing logic operation NAND or NOR. In both the last cases the NOT-operation can be obtained by fixing one of the gate's inputs at the level 0 or 1.

In an ideal sense, the nonlinear input-output functions should be step-like threshold functions, whose threshold's altitude corresponds to two different levels in logic operation.

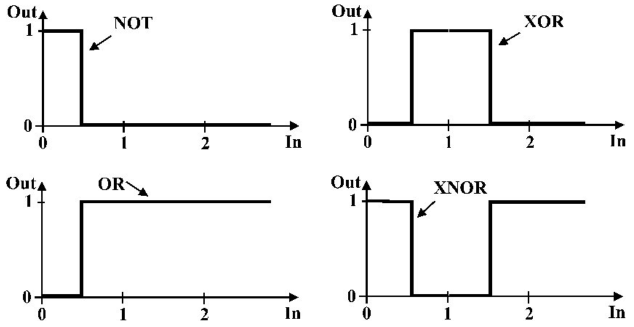

FIGURE 2. Nonlinear input-output functions with two-inputs, realizing some binary logic operations.

We present the results of our investigations in the field of creating novel opto-electronic components for digital computing, founded on acousto-optical interaction in bulk crystals. The case at hand is to present some of the input-output characteristics for the logic operations in optics via the mechanism of a two-phonon light scattering in anisotropic medium. Such an approach is promising to achieve a high-bit rate, conditioned by an all-optical scheme of governing the light by light, together with a possibility for designing a matrix arrangement of digital processor because of advanced acousto-optic technology.

2. General consideration

Now, there is a good reason to take an advantage of the quantum approach to the phenomenon under consideration, which can be interpreted as scattering the light quanta-photons by the quanta of acoustic field-phonons. When the length of interaction is large enough, it is reasonable to believe that the phonons are passing through infinite medium and, consequently, they have well-determined magnitude of the momentum. Thus, one may use the conservation laws for both the energy and the momentum

$$\omega_1 = \omega_0 \pm \Omega, \quad \overrightarrow{k_1} = \overrightarrow{k_0} \pm \overrightarrow{K}, \tag{1}$$

where ω_1, ω_0 and $\overrightarrow{k_0}, \overrightarrow{k_1}$, are the angular frequencies and wave vectors of interacting light waves, respectively; while Ω and $\overrightarrow{K}$ are the angular frequency and wave vectors of phonon. In Eqs. (1), the plus sign corresponds to originating an anti-Stokes photon, whereas the minus sign meets a Stokes photon. By this it means that there are two processes, manifesting the annihilation of a phonon (anti-Stokes process) or origination of a Stokes phonon. Under conventional experimental conditions, when intensities of light and acoustic beams are approximately equal to each other, the number of phonons is 10^5 times more than the number of photons, and up to 100% of photons can be scattered due to three-particle processes without appreciable effect on a stream of acoustic phonons. Consequently, the process of light scattering by coherent acoustic phonons can be considered in approximation of a prescribed phonon field.

Over the long run, the linkage between wave vectors of interacting particles can be expressed in the form of wave vector diagrams on cross-sections of the wave vector surfaces inherent in a crystal. Similar diagrams represent a graphic version of the conservation laws, see Eqs. (1), and they may be exploited for the analysis of scattering. For example, Fig. 3a illustrates an opportunity for one-fold scattering of the incident photon by one acoustic phonon in a single-axis crystal, when the initial and ultimate states of polarization for these photons are different.

Then, under certain conditions, *i.e.*, at set angles of light incidence on the phonon beam and at fixed angular frequencies of phonons, one can observe the phenomenon of two-fold scattering of light caused by participating two acoustic phonons.

The main peculiarity of this phenomenon lies in conserving both the energy and the momentum for two transitions simultaneously. In their own turn, these laws determine the angular frequencies and wave vectors of all three interacting waves:

$$\begin{aligned} \omega_1 &= \omega_0 \pm \Omega, & \overrightarrow{k_1} &= \overrightarrow{k_0} \pm \overrightarrow{K}, \\ \omega_2 &= \omega_0 \pm 2\Omega, & \overrightarrow{k_2} &= \overrightarrow{k_0} \pm 2\overrightarrow{K}, \end{aligned} \tag{2}$$

where ω_p and $\overrightarrow{k_p} (p = 0, 1, 2,)$ the angular frequencies and wave vectors of interacting photons. This fact leads to originating two orders of scattering, apart the zero-th one, each by itself satisfies the conservation laws, described by Eqs. (2). Figure 3b presents the diagram of wave vectors, dealing with a two-phonon scattering of light quanta in a uniaxial crystal. Such a diagram offers rather small angles of deflection and occurs at the specific angular frequency of acoustic phonons, peculiar to just a two-phonon scattering, which can be determined as

$$\Omega = 2\pi\lambda^{-1} v \sqrt{|n_0^2 - n_1^2|}, \tag{3}$$

here n_p is the corresponding refractive index, so $n_0 \approx n_2 \neq n_1$.The polarization of light in the zero-th and the second orders is orthogonal to the polarization of light in the first order, whereas the carrier frequencies of light beams in the first and the second orders are shifted Ω and 2Ω, respectively, with reference to the zero-th order.

3. A two-phonon scattering of light

Now we can use this approach to Bragg regime, and propose a new regime when the direct transitions are allowed between

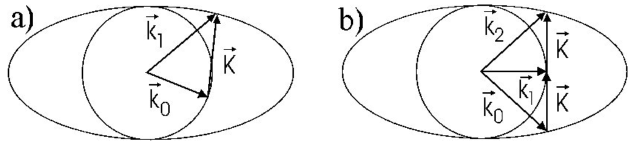

FIGURE 3. Wave vector surfaces and wave vector diagrams inherent in one-fold (a) and two-fold (b) scattering of photon by acoustic phonons in a single-axis crystal.

all optical modes in a bulk crystal. When the perfectly polarized plane light wave propagates through in a crystal, wherein two plane elastic waves with the angular frequencies Ω and 2Ω as well as with wave numbers K and $2K$, respectively, are passing along the z-axis, whose perturbed refractive index is (See Fig. 4).

$$n = n_0 + \Delta n_1 \sin(Kz - \Omega t) + \Delta n_2 \sin(2Kz - 2\Omega t)\,. \quad (4)$$

Here n_0 is a non-perturbed refractive index in the approximation of $n_0 \approx n_1$; Δn_1 and Δn_2 are the amplitudes of perturbations. Let us assume that the area of propagation for the elastic wave is bounded by two planes $x = 0$ and $x = L$, so it is arranged in acoustic beam, and that the plane electromagnetic wave

$$E = E_0 \exp\left[i\left(k_0 x \cos(\theta_0) + k_0 z \sin(\theta_0) - \omega_0 t\right)\right], \quad (5)$$

strikes the plane $x = 0$ at the angle θ_0 to the x-axis. Here E_0 is the amplitude of incident wave, ω_0 and $k_0 = 2\pi\lambda^{-1}n_0$ are the angular frequency and the wave number, λ is the wavelength of incident light. Without the loss in generality, one may put that all the fields are independent of the coordinate y, so a scalar wave equation, governing the electric component $E(x, y, z, t)$ of electromagnetic wave in $x \in [0, L]$ the area of interaction, has the following form $C_p(x)$

$$\frac{\partial^2 E}{\partial x^2} + \frac{\partial^2 E}{\partial z^2} - \frac{1}{c^2}\frac{\partial^2(\epsilon E)}{\partial t^2} = 0, \quad (6)$$

here $\epsilon = n^2(z, t)$ is the dielectric constant in the medium with acoustic beam present. Since $\Delta n_p \ll n_0$ were $p = 1, 2$ in Eq. (4), one can write

$$\epsilon(z, t) \approx n_0^2 + n_0 \Delta n_1 \sin(Kz - \Omega t + \Phi_1) + n_0 \Delta n_2 \sin(2Kz - 2\Omega t + \Phi_2)\,. \quad (7)$$

Only two, the first and the fourth summands, belonging to the expansion of dielectric constant into a series in terms of a small external perturbation, are taken into account in Eq. (7). Let us represent the project of solution to Eq. (6) in the area as a sum of partial waves with the amplitudes

$$E = E_0 \sum_{p=0}^{2} C_p(x) \exp\left[i\left(k_{p,x} x + k_{p,z} z - \omega_p t\right)\right], \quad (8)$$

where

$$\omega_p = \omega_0 + p\Omega, \qquad k_p = |\overrightarrow{k_p}| = \omega_p \sqrt{\epsilon_0}\, c^{-1},$$
$$k_{p,x} = \sqrt{k_p^2 - k_{p,x}^2}.$$

The equation (8) does not contain any reflected waves. This may be tolerated, because a comprehensive analysis shows that usually the length for coherent interaction between co-directional waves far exceeds the same length for oppositely directed waves. The reflected waves become to be essential when the scattering angles are close to 90°. A total number of summands in Eq. (8) is already finite, and it increases as the ratio K/k_0 decreases. In the chosen approximation, we obtain the following set of ordinary differential equations

$$\frac{dC_p}{dx} = q_p\left\{C_{p-1}\exp\left[i\left(\eta_{p-1}x + \Phi\right)\right] - C_{p+1}\exp\left[-i\left(\eta_p x + \Phi\right)\right]\right\} + r_p\left\{C_{p-2}\exp\left[i\left(\xi_{p-2}x + \Phi\right)\right] - C_{p+2}\exp\left[i\left(\xi_p x + \Phi\right)\right]\right\}, \quad (9)$$

where

$$q_p = \Delta n_1 k_p (2n_0)^{-1}, \qquad \eta_p = k_{p,x} - k_{p+1,x},$$
$$r_p = \Delta n_2 k_p (2n_0)^{-1}, \quad \text{and} \quad \xi_p = k_{p,x} - k_{p+2,x}.$$

It follows from Eq. (9), that the redistribution of energy in each p-th order of scattering is governed by the only neighboring orders with numbers $p \pm 1$ and $.p \pm 2$ The second derivatives $d^2 C_p/dx^2$ were discarded, which is directly correlated with ignoring the waves reflected.

To extend the obtained equations rigorously to anisotropic media, broadly speaking, proper allowance must be made for the tensor description of dielectric properties inherent in such media. This is intimately related to the fact that Bragg scattering with changing the polarization of light is feasible in anisotropic media. Nonetheless, Eq. (9) may be applied to analyzing the light scattering in anisotropic media under certain refinements. Because usually some concrete process is of chief interest, we need only to reinterpret the parameters q and r entering into Eq. (9) and describing the efficiency of interaction. With due regard for this procedure Eq. (9) have the ability of governing the taken alone process in anisotropic media wholly adequately. First, one can disregard all the amplitudes $C_p(x)$ in Eq. (9) with the exception of the amplitudes C_0, C_1, and C_2. Second, when a two-phonon light scattering is realized, it is seen from the wave vector diagram in Fig. 4a that $\eta_p = \xi_p = 0$. Consequently, in the case of stationary scattering we obtain the following set of

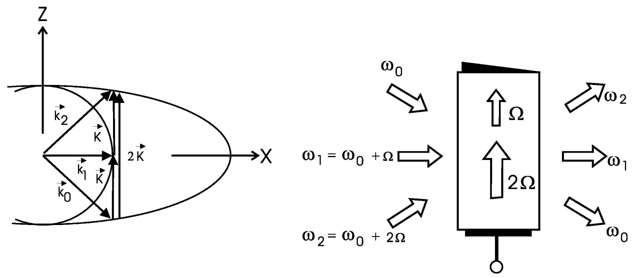

FIGURE 4. The wave vector diagram and schematic arrangement for a two-phonon light scattering in a uniaxial crystal, allowing direct transitions between all the light modes.

simplified ordinary differential equations for the amplitudes of light modes

$$\frac{dC_0}{dx} = -qC_1 - rC_2, \quad \frac{dC_1}{dx} = q(C_0 - C_2),$$
$$\frac{dC_2}{dx} = qC_1 + rC_0. \tag{10}$$

Here the approximate relations $q_0 \approx q_1 \approx q_2 \approx q$ and $r_0 \approx r_2 \approx r$ are substituted, into Eq. (10). It may be tolerated on above-mentioned assumption that the shifts in carrier angular frequencies of light waves, included in the amplitude coefficients for different orders, can be neglected. All the parameters q_p with $p = 0, 1, 2$ describe the efficiency of interaction, changing the polarization state of light, as well as the parameters r_p with $p = 0, 2$ are intrinsic to the interaction with no changing the polarization. In the general case $q_p \neq r_p$, because these two types of scatterings are provided by different photo-elastic constants. The exact and closed analytical solutions to Eq. (10) with the stationary boundary conditions

$$C_0(x=0) = A_0 \exp(i\varphi_0), \quad C_1(x=0) = A_1 \exp(i\varphi_1),$$
$$\text{and} \qquad C_2(x=0) = A_2 \exp(i\varphi_2),$$

where A_0, A_1, A_2 and φ_0, φ_1, φ_2 are the amplitudes and phases of incident light waves on the plane $x = 0$, have the form

$$C_0(x) = \left(2q^2 + r^2\right)^{-1} \Big\{ 2\left[q^2 A_2 \exp(i\varphi_2) - qrA_1 \exp(i\varphi_1)\right] \sin^2\left(\frac{x}{2}\sqrt{2q^2+r^2}\right) - \sqrt{2q^2+r^2}\,[qA_1 \exp(i\varphi_1)$$
$$+ rA_2 \exp(i\varphi_2)] \sin\left(x\sqrt{2q^2+r^2}\right) + \left[2q^2 \cos^2\left(\frac{x}{2}\sqrt{2q^2+r^2}\right) + r^2 \cos\left(x\sqrt{2q^2+r2}\right)\right] A_0 \exp(i\varphi_0) \Big\}, \tag{11}$$

$$C_1(x) = \left(2q^2 + r^2\right)^{-1} \Big\{ A_1 \exp(i\varphi_1) \left[r^2 + 2q^2 \cos\left(x\sqrt{2q^2+r^2}\right)\right] - 2qr\,[A_0 \exp(i\varphi_0)$$
$$+ A_2 \exp(i\varphi_2)] \sin^2\left(\frac{x}{2}\sqrt{2q^2+r^2}\right) + q\left(\sqrt{2q^2+r^2}\right) [A_0 \exp(i\varphi_0) - A_2 \exp(i\varphi_2)] \sin\left(x\sqrt{2q^2+r^2}\right) \Big\}, \tag{12}$$

$$C_2(x) = \left(2q^2 + r^2\right)^{-1} \Big\{ 2\left[q^2 A_0 \exp(i\varphi_0) - qrA_2 \exp(i\varphi_2)\right] \sin^2\left(\frac{x}{2}\sqrt{2q^2+r^2}\right) + \left(\sqrt{2q^2+r^2}\right) [qA_1 \exp(i\varphi_1)$$
$$+ rA_0 \exp(i\varphi_0)] \sin\left(x\sqrt{2q^2+r^2}\right) + \left[2q^2 \cos^2\left(\frac{x}{2}\sqrt{2q^2+r^2}\right) + r^2 \cos\left(x\sqrt{2q^2+r^2}\right)\right] A_2 \exp(i\varphi_2) \Big\}. \tag{13}$$

Equations (11-13) make it possible to analyze a three-order acousto-optical interaction, having regard to direct transitions between all the light modes. The transition probabilities are electronically controllable and they may be varied within wide limits according to the level of incoming power density in elastic waves. For further analysis Eqs. (11-13) can be rewritten in terms of the intensities, *i.e.*, we shall consider the intensities $|C_p(x)|^2$ as functions of the coordinate x and exploit the value r as a parameter, with the incoming light intensities A_p^2 and the initial phases φ_p chosen in a specific way. For simplicity sake the cases are chosen, when the only one incoming light intensity has a non-zero magnitude. If $A_i^2 = 1$, $q = 1$, and $\varphi_i = 0$, while $A_j^2 = A_k^2 = 0$ $(i \neq j \neq k, i, j, k = 0, 1, 2)$, we arrive at a set of diagrams shown in Fig. 5. The value of $r = 0$ corresponds to the conventional approach to a three-order acousto-optical interaction [7,8], wherein the only two-phonon scattering provides the coupling between the zero-th and the second orders, and the intensity $|C_1(x)|^2$ does not exceed 50% of the incoming light intensity A_0^2. Nevertheless, with $r \neq 0$ one can increase the portion of light, scattered into the first order, so it is clearly seen from Fig. 5a that up to 100% of the incoming light intensity can be deflected into the first order when the optimal magnitude of $r = 1$ is taken. Besides that, the spatial shifts of the intensity maxima in both another orders are observed. Thus, we have obtained exact and closed analytical description for a three-order acousto-optical interaction, having regard to direct transitions between all the light modes. In this case the physical scheme of light scattering can be easily realized using the scheme of conventional a two-phonon acousto-optical interaction and inserting the second elastic wave, whose frequency has to be twice as high as the main one, see Fig. 3b. The relative contribution of a direct coupling between two extreme orders is revealed and it can be optimized from the viewpoint of increasing the light intensity in previously decayed orders of scattering.

4. Performing the logic operations

The elementary components of digital circuits are usually made up of combinational elements such as NAND and NOR logic gates and memory elements, which might be single bit memory elements such as discrete flip-flops. They are composed of transistors as electrically active elements. The two most frequently used kinds of transistors are the bipolar and the field effect transistors [9]. In this chapter we are applying the phenomenon of scattering the light by ultrasound to de-

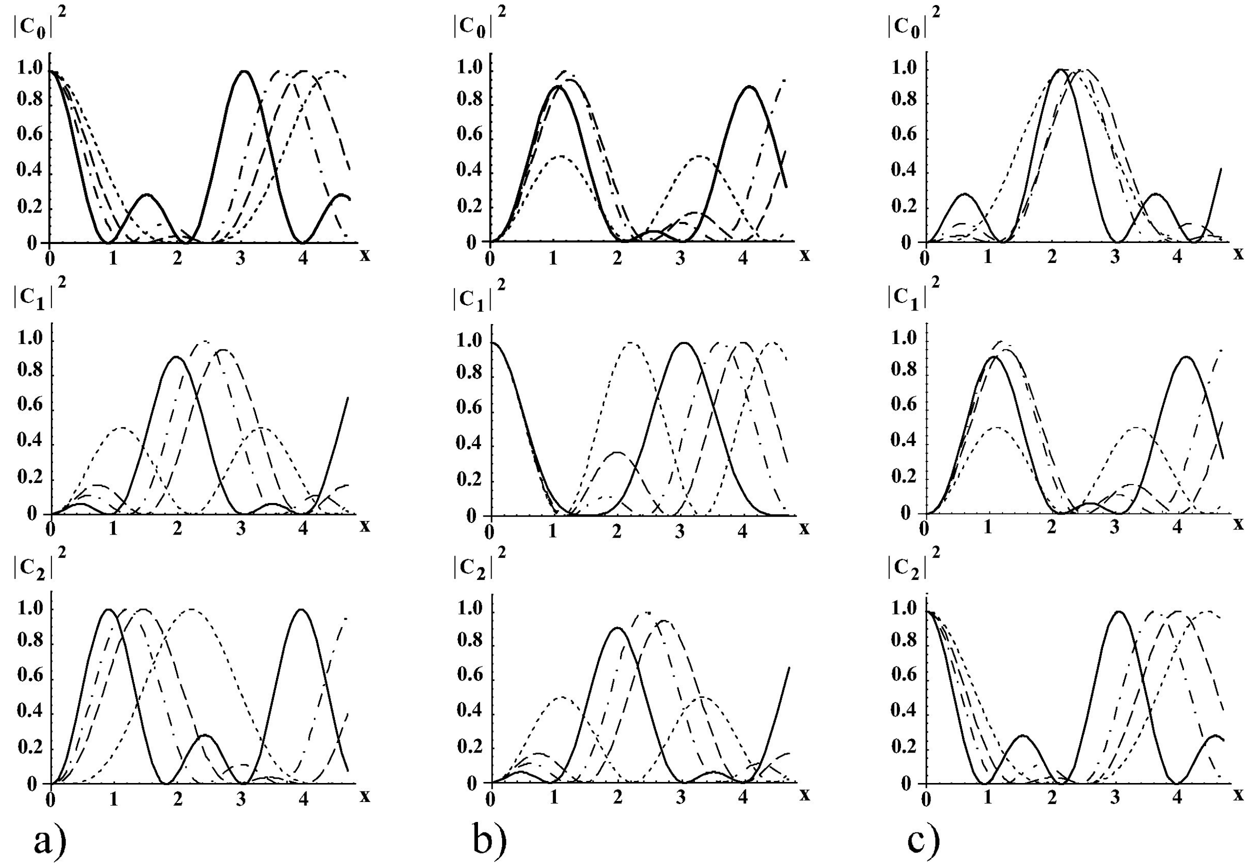

FIGURE 5. The intensities of scattered light waves versus the coordinate x:

a) $C_0(x=0)=1$; $C_1(x=0)=0$; $C_2(x=0)=0$,

b) $C_0(x=0)=0$; $C_1(x=0)=1$; $C_2(x=0)=0$;

c) $C_0(x=0)=0$; $C_1(x=0)=0$; $C_2(x=0)=1$.

The dotted lines are for r = 0; the dashed lines are for r = 0.7; the dot-dashed lines are for r = 1.0; the solid lines are for r = 1.5.

sign all-optical logic gates. The approach to creating similar components can be demonstrated by the example of a two-phonon light scattering, the analysis of Eqs. (11-13) permits realizing such a lot of logic operations with or without optical pump. It is convenient to denote the corresponding acousto-optical processes as $i \xrightarrow{m} j$, $i+j \longrightarrow k$ or $i+j \xrightarrow{m} k$, where the orders of input and output light beams appear on the left and right, while the order of pump beam is indicated above the arrows.

First we discuss the technique of creating the logic gate, having only one input and one output. Such a gate exists and it realizes the logic operation NOT. In the case of a two-phonon light scattering a few optical schemes can be exploited for designing such a gate. For instance, we can take the process $0 \xrightarrow{1} 0$. In this case, so one can obtain from Eqs. (11)

$$|C_0(L)|^2 = A_0^2 \cos^4\left(\frac{qL}{2\sqrt{2}}\right) + \frac{A_1^2}{2}\sin^2\left(\frac{qL}{\sqrt{2}}\right) - \sqrt{2}A_0A_1\cos^2\left(\frac{qL}{2\sqrt{2}}\right)\sin\left(\frac{qL}{\sqrt{2}}\right)\cos\left(\varphi_0-\varphi_1\right). \quad (14)$$

Here the beam A_0 corresponds to a signal channel, while the beam A_1 represents a pump. It follows from the truth table for the NOT-gate that $|C_0(L)|^2 = 1$ with $A_0 = 0$, so $(A_1^2/2)\sin^2(qL/\sqrt{2}) = 1$. Then, $|C_0(L)|^2 = 0$ with $A_0 = 1$, and we arrive at the formula

$$\cos^4\left(\frac{qL}{2\sqrt{2}}\right) + 1 - 2\cos^2\left(\frac{qL}{2\sqrt{2}}\right)\cos(\varphi_0 - \varphi_1).$$

Setting $\varphi_0 = \varphi_1$, we yield $\cos^2(qL/2\sqrt{2}) = 1$ and

$$\left(\frac{qL}{2\sqrt{2}}\right) = \{0 \pm \pi, \pm 2\pi, \ldots\}.$$

This means that

$$\left(\frac{qL}{\sqrt{2}}\right) = \{0 \pm \pi, \pm 2\pi, \pm 4\pi, \ldots\},$$

so $\sin^2(qL/\sqrt{2}) \longrightarrow 0$ and $A_1 \longrightarrow \infty$, when

$$\left(\frac{qL}{\sqrt{2}}\right) \longrightarrow \{0 \pm \pi, \pm 2\pi, \pm 4\pi, \ldots\}.$$

This theoretical requirement needs practical interpretation, because the product $(A_1^2/2)\sin^2(qL/\sqrt{2}) = 1$ is determined not quite well. Of course, the value $qL = 0$ is not acceptable due to decreasing the thickness of crystal or the level of acoustic power, or both. While, for instance, with $qL \to 2\sqrt{2}\pi$ we arrive at the conclusion that the more will be the pump A_1 the closer will be the boundary states of NOT logic gate to 0 or 1, respectively. The dependence of the output intensity $|C_0(L)|^2$ on the signal beam intensity A_0^2 in the form $|C_0(L)|^2 = (1 - A_0)^2$, representing in fact the input-output characteristic of the NOT-gate under consideration, is shown in Fig. 6. The same kind of consideration can be performed in connection with performing the NOT-logic operation for another process of the $i \xrightarrow{m} j$ type as well. Thus, the mechanism of a two-phonon light scattering can be successfully exploited for designing the NOT logic gate with a pump, whose intensity transmission coefficient is practically equal to 100%.

Now, we are coming to the question of applying the scheme of a two-phonon light scattering to the performing of logic operations with two inputs and two outputs under requirement for the input beams to be functionally indistinguishable. When the pump is absent, the processes of the $i + j \longrightarrow k$ type can be realized, so one can take, for example, the process $0 + 2 \longrightarrow 1$. In this case $A_1 = 0$; the beams A_0 and A_2 correspond to two input signal channels, while the beam C_1 represents the output channel. Consequently, it follows from Eqs. (11) that

$$|C_1(L)|^2 = \frac{1}{2}\sin^2\left(\frac{qL}{\sqrt{2}}\right) \times \left[A_0^2 + A_2^2 - 2A_0A_2\cos(\varphi_0 - \varphi_2)\right]. \quad (15)$$

Here, we may put $\sin^2(qL/\sqrt{2}) = 1$ and meet two possibilities. The first one lies in the condition $\varphi_0 = \varphi_2$, so we arrive at the XOR-logic gate whose input-output characteristic has the form $|C_1(L)|^2 = (1/2)(A_0 - A_2)^2$. The second possibility complies with $\varphi_0 - \varphi_2 = \pi/3$ and $\cos(\varphi_0 - \varphi_2) = 1/2$. In this case we yield the OR-logic gate with the following input-output characteristic: $|C_1(L)|^2 = \frac{1}{2}(A_0^2 + A_2^2 - A_0A_2)$. Both these characteristics are presented in Fig. 7. It is seen from the last-mentioned formulae and Fig. 7 that the intensity transmission coefficients in these logic gates are equal to 50% due to the absence of a pump.

Finally, we have to consider the application of a two-phonon light scattering to performing logic operations via various processes of the $i + j \xrightarrow{m} k$ type with a pump. For this purpose the process $0 + 2 \xrightarrow{1} 1$ will be used. In this case the beams A_0 and A_2 correspond to two input signal channels, the beam C_1 represents the output channel and $A_1 \neq 0$. We may put $\varphi_1 = 0$ and rewrite from Eqs. (12)

$$|C_1(L)|^2 = \frac{1}{2}\sin^2\left(\frac{qL}{\sqrt{2}}\right)\left(A_0^2 + A_2^2\right) + A_1\cos^2\left(\frac{qL}{\sqrt{2}}\right) - A_0A_2\sin^2\left(\frac{qL}{\sqrt{2}}\right)\cos(\varphi_0 - \varphi_2) - \sqrt{2}A_1\sin\left(\frac{qL}{\sqrt{2}}\right)\cos(A_0\varphi_0 - A_2\varphi_2). \quad (16)$$

The same sort of analysis as before shows that the process $0 + 2 \xrightarrow{1} 1$ allows performing, in particular, the XNOR-logic

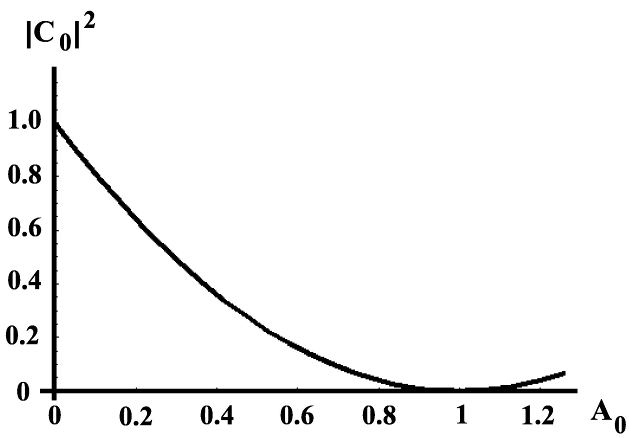

FIGURE 6. The input-output characteristic for the NOT-logic gate with a pump.

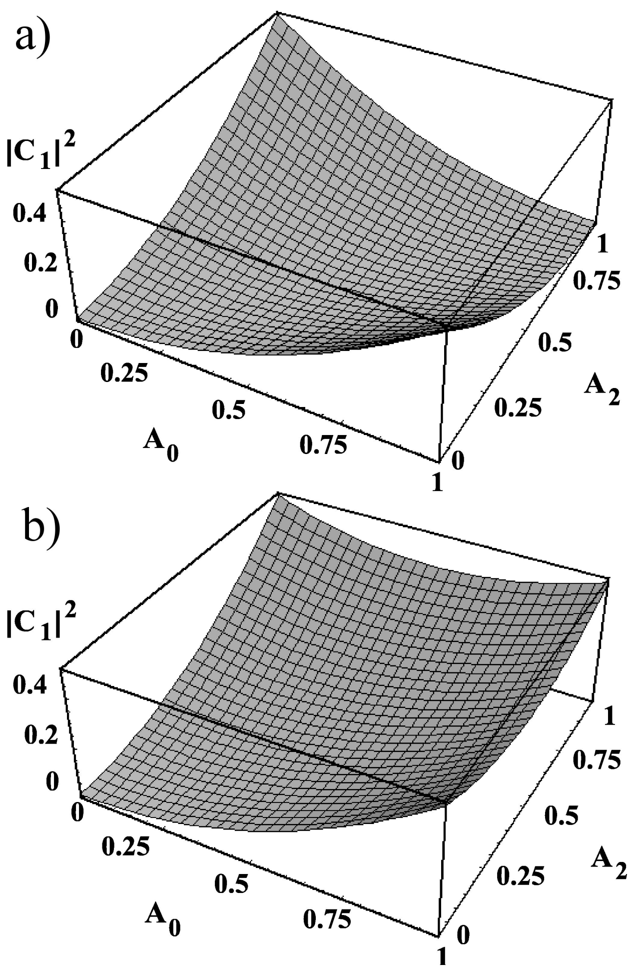

FIGURE 7. The input-output characteristics of the logic gates: a) XOR and b) OR.

operation. To make the input beams functionally indistinguishable, we have to symmetrize Eq. (12) relative to the contributions of the input amplitudes A_0 and A_2 and ought to put $\varphi_0 = \varphi_2 + \pi$. When $A_0 = A_2 = 0$, Eq. (16) gives

$$|C_1(L, A_0 = 0, A_2 = 0)|^2 = A_1^2 \cos^2\left(\frac{qL}{\sqrt{2}}\right) = \eta^2, \quad (17)$$

where η^2 is the intensity transmission coefficient. It should be noted that the presence of optical pump with $A_1 \neq 0$ makes it possible to generate the output signal even when both the input signals are equal to zero, and to perform the XNOR-logic operation. From the truth table for the XNOR-logic gate we know that

$$|C_1(L, A_0{=}0, A_2 = 0)|^2 = |C_1(L, A_0{=}0, A_2 = 1)|^2 = 0$$

and

$$|C_1(L, A_0 = 1, A_2 = 1)|^2 = \eta^2,$$

using Eq.(17), we calculate

$$\frac{1}{2}\sin^2\left(\frac{qL}{\sqrt{2}}\right) + \eta^2 - \sqrt{2}\eta \sin\left(\frac{qL}{\sqrt{2}}\right)\cos(\varphi_0) = 0, \quad (18)$$

$$2\sin^2\left(\frac{qL}{\sqrt{2}}\right) + \eta^2 - 2\sqrt{2}\eta \sin\left(\frac{qL}{\sqrt{2}}\right)\cos(\varphi_0) = \eta^2, \quad (19)$$

The solution: $\sin^2(qL/\sqrt{2}) \longrightarrow 1$, $\eta \longrightarrow (1/\sqrt{2})$, $\cos(\varphi_0) = \pm 1$ leads to: $A_1 \longrightarrow \infty$ with $\cos^2(qL/\sqrt{2}) \longrightarrow 0$. The input-output characteristic of the XNOR-logic gate can be written as $|C_1(L)|^2 = (1/2)(1 - A_0 - A_2)^2$, see Fig. 8, so the intensity transmission coefficient of this logic gate is equal to 50%. The last value is conditioned by the properties of a two-phonon light scattering and can be, probably, improved with changing the regime of acousto-optical interaction. All these logic gates are interferometric in behavior; that is why they have the ability to control over faint light streams and the level of the order of 10^{-15} J/bit may estimate this restriction.

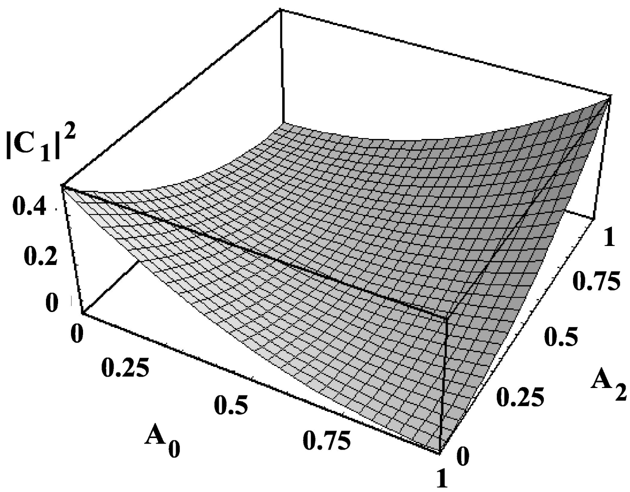

FIGURE 8. The input-output characteristic for the XNOR-logic gate with an optical pump.

5. All-optical implementation of key component for the J-K flip-flop

In addition to logic gates, a digital system uses many other functional modules built on gates, these include the bistable multivibrator or one-shot, and the astable multivibrator or free running clock. The multivibrator circuit can be represented by using MIL-STD-806B symbols as shown in Fig. 9. The flip-flop is simply a digital memory device that can store only one "bit" at a time [10]. To explain this we use the SR flip-flop shown symbolically in Fig. 9, the set and reset inputs being labeled S and R respectively, and the complementary outputs are labeled Q and $\overline{Q}$. The state table for the flip-flop is shown in the Table I. in the first three columns of this table all combinations of the presented states of S, R and Q are shown, *i.e.*, their states at time t, the fourth column contains a tabulation of the next state of the flip-flop, *i.e.*, its state at time $t + \Delta t$. The examination of this table shows that a change of flip-flop state occurs in the rows 4 and 5 only, in the row 4 the flip-flop is being reset or turned off, *i.e.*, its state is changing from 1 to 0 as a consequence of the of the application of a reset input $R = 1$. In the row 5 the flip-flop is being set or turned on, *i.e.*, its state is changing from 0 to 1 as a result of the application of a set input $S = 1$. For the rows 1 and 2, $S = 0$ and $R = 0$, and consequently there is no change in the state of the flip-flop and the entries in the last column are 0 and 1 respectively. On the row 3, $R = 1$ and the signal in normal circumstances would turn the flip-flop off, however the flip-flop is already turned off since $Qt = 0$ and consequently the signal $R = 1$ leaves the flip-flop state unchanged. Similarly in the row 6, $S = 1$, and this signal would normally turn the flip-flop on, but when $Qt = 1$, *i.e.*, the flip-flop is already turned on and consequently there will be no change the state of the flip-flop, Finally with this type of flip-flop it is forbidden for S and R to be logical '1' simultaneously, this restriction being expresses algebraically by $SR = 0$. In the other hand the Fig. 10 shows the symbolic representation of the JK flip-flop and the table 2 describe the logical operation. The operation of this flip-flop differs in one respect from that of the SR flip-flop in that is allowable for J and K to be simultaneously equal to logical '1'. For example, if $J = K = 1$, the flip-flop 'toggles', that is, in the row 7 the flip-flop changes the state from 0 to 1 while in the row 8 the converse action takes place. In the rows 4 and 5 normal reset and set operations take place as described for the SR flip-flop [10].

TABLE I. Simplified truth table for the S-R flip-flop.

Actual state			Next state	Actual state			Next state
S	R	Qt	$Qt+\Delta t$	S	R	Qt	$Qt+\Delta t$
0	0	0	0	1	0	0	1
0	0	1	1	1	0	1	1
0	1	1	0	1	1	0	Forbidden
0	1	0	0	1	1	1	Combination

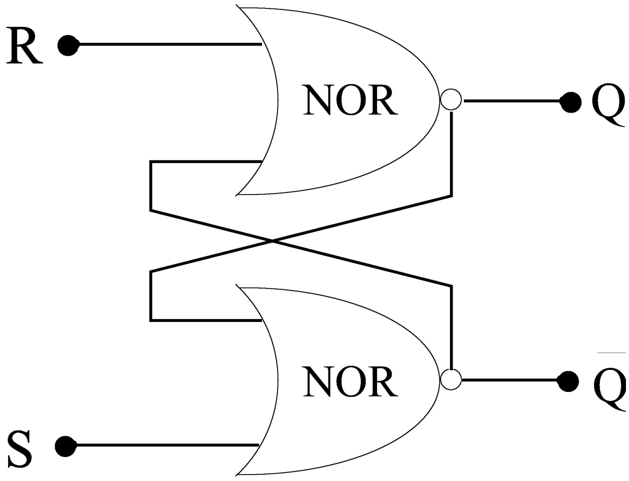

FIGURE 9. The cross-coupled flip-flop based on tow NOR gates.

This circuit actually contains two cross-connected resistor NOR-gates, where one NOR gate has as Q output, and R and $\bar{Q}$ as inputs, while the other NOR gate has S and Q as inputs, and $\bar{Q}$ as output. Due to its configuration, this circuit is also called a cross-coupled flip-flop [10].

Of course, to manifest optical bistability any digital device should include a feedback. However, for the sake of simplicity we will consider here the only key component of the J-K flip-flop leaving aside the problem of arranging an all-optical feedback. Let us consider the implementation of key component for an all-optical J-K flip-flop, whose switching properties are reflected in Table II.

TABLE II. Simplified truth table for the J-K flip-flop.

Actual state			Next state	Actual state			Next state
J	K	Qt	$Qt+\Delta t$	J	K	Qt	$Qt+\Delta t$
0	0	0	0	1	0	0	1
0	0	1	1	1	0	1	1
0	1	0	0	1	1	0	1
0	1	1	0	1	1	1	0

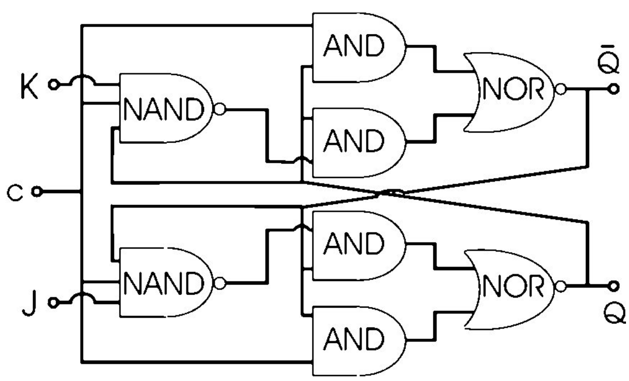

FIGURE 10. Representation of the J-K flip-flop.

We present the exact analytical description for such an innovated regime and then, using computer simulation, analyze the feasibilities of its application to performing binary logic-based operations for all-optical switching. In order to implement the key component for an all-optical J-K flip-flop, we have to search for optical scheme of device and to optimize the normalized length L of scattering. We have proposed two schematic arrangements of the key component for the J-K flip-flops (see Fig. 11). Analysis has shown that one can select the beam $A_1 = 1$ for the optical pump and the beams A_0 and A_2 for all-optical inputs, while the beams $C_0(L)$, $C_1(L)$, and $C_2(L)$ represent the output beams, as the case requires. In so doing, we arrive at the desired truth tables for the key components conditioned by the lengths L selected, see Table III.

TABLE III. Truth tables for two implementations of the J-K flip-flop's key components, associated with Fig.11.

Input J	Input K	Optical outputs at $L = 2\pi/3\sqrt{3}$			Input K	Input J	Optical outputs at $L = 4\pi/3\sqrt{3}$		
A_0	A_2	Qt	$Qt+\Delta t$	$\overline{Q}$	A_0	A_2	Qt	$Qt+\Delta t$	$\overline{Q}$
0	0	0	0	0	0	0	0	0	0
0	1	0	0	1	0	1	0	1	0
1	1	0	1	1	1	1	0	1	1
1	0	0	1	0	1	0	0	0	1

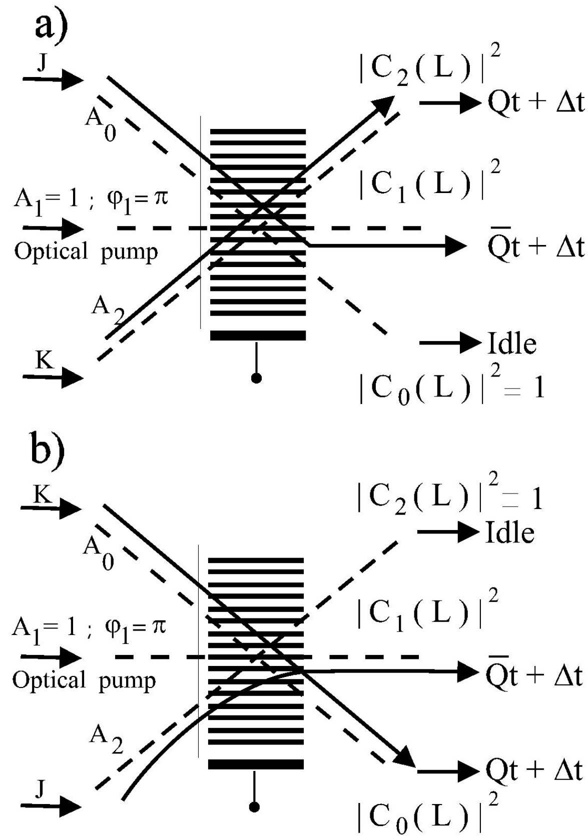

FIGURE 11. All-optical implementations of key components for the J-K flip-flops with: a) $L = 2\pi/3\sqrt{3}$, b) $L = 4\pi/3\sqrt{3}$.

6. Conclusion

We have covered some peculiarities inherent in a two-phonon scattering of light in anisotropic media. For this purpose, the approach based on analyzing the conservation laws and describing the evolution of light waves has been exploited. The possibility of applying a two-phonon light scattering to designing some input-output characteristics for the logic operations in optics has been considered.

We can see the behavior of the input-output characteristics shown in the Fig. 2, and compare directly with our analytic result in connection with the 3D-plots for the NOT, OR, XOR and XNOR. The simulation for the NOT input-output characteristic shown that we can obtain up to 100% of efficiency of the scattered light, but for the next three 3D-plots we can obtain only the 50% of efficiency in comparison with the input-output characteristics shown in the Fig. 2. This problem is attached to the properties of the acousto-optical interaction.

The obtained results involve a few all-optical arrangements for designing the key component of the J-K flip-flop, which have been algorithmically estimated. The direct transitions make it possible to provide an all-optical switching with the efficiency of about 100%.

Acknowledgements

This work was financially supported by the CONACyT (Project # PY33074-E) and the INAOE (Opto-Electronic Project).

1. F. Yu. *Introduction of information optics* (Academic Press, San Diego, 2001).
2. H.M. Gibbs, *Optical bistability: controlling the light with light* (Academic Press, Orlando, 1985).
3. E.A. Kuzin *et al.*, *J.Opt.Soc.Am. B.* **14** (1997) 1345.
4. A.S. Shcherbakov and V. Yu.Rakovsky, *Proc. SPIE.* **3238** (1997) 167.
5. R. Hainberger *et al.*, Special Issue on Optical Interconnects/Optical Signal Processing, *IEICE Trans. Electron* **E84-C** (2001) 358.
6. D.N. Maywar and G.P. Agrawal, *Optics Express* **3** (1998) 440.
7. V.I. Balakshy, V.N. Parygin, and L.I. Chirkov, *Physical Principles of Acousto-Optics* (Radio i Svyaz, Moscow, 1985).
8. A. Korpel, *Acousto-Optics* (Marcel Dekker, New-York, 1988).
9. N. Wirth, *Digital circuit desing for computers science students* (Springer-Verlag, Berlin, 1995).
10. J.D. Daniels, *Digital design from zero to one* (John Wiley, New York, 1996).